

See discussions, stats, and author profiles for this publication at: <https://www.researchgate.net/publication/231632768>

Theoretical Study of the Quadrupolarity of Carbodiimide†

ARTICLE *in* THE JOURNAL OF PHYSICAL CHEMISTRY A · AUGUST 2002

Impact Factor: 2.69 · DOI: 10.1021/jp020553r

CITATIONS

12

READS

24

3 AUTHORS, INCLUDING:



Rainer Glaser

University of Missouri

159 PUBLICATIONS 2,559 CITATIONS

SEE PROFILE



Zhengyu Wu

Renmin University of China

22 PUBLICATIONS 149 CITATIONS

SEE PROFILE

Theoretical Study of the Quadrupolarity of Carbodiimide[†]

Rainer Glaser,* Michael Lewis, and Zhengyu Wu

Department of Chemistry, University of Missouri-Columbia, Columbia, Missouri 65211

Received: February 27, 2002; In Final Form: June 4, 2002

The quadrupolarity of carbodiimide, $\text{HN}=\text{C}=\text{NH}$, has been studied in comparison to carbon dioxide. Both heterocumulenes exhibit $\{- + -\}$ quadrupolarity in all directions. Concepts are formulated to develop an understanding of the origins of quadrupole moments and to trace theoretical level effects to the underlying changes of the electron density. The quadrupole moment tensors have been computed using RHF, MP2 and QCISD theory as well as the B3LYP density functional method. A variety of basis sets have been employed, the two best basis sets are of the types $[5s, 4p, 2d, 1f]$ (23s, 8p, 2d, 1f) and $[5s, 4p, 3d, 1f]$ (12s, 6p, 3d, 1f). The results suggest that the MP2 and B3LYP methods in conjunction with well-polarized triple- ζ basis sets provide a cost-effective and quite accurate method for the estimation of correlation effects on quadrupole moments. The quadrupole moment tensor component Q_{xx} of carbodiimide falls between -16 and -18 D \AA . The components Q_{yy} and Q_{zz} , are similar and they range from -16.5 to -17.5 D \AA and from -17 to -18 D \AA . The correlated methods consistently predict an increase of Q_{xx} , whereas they predict a more modest reduction of Q_{yy} and Q_{zz} . It is for these opposing correlation effects that the average values of the diagonal elements, $\langle Q_{ii} \rangle$, are essentially independent of the method and exhibit only a minor basis set dependence. The traceless quadrupole moment of carbon dioxide, $\Theta = Q_{||} - Q_{\perp}$, is -4.3 D \AA . In stark contrast, all of the Θ_{ii} values of carbodiimide are close to zero and only the off-diagonal quadrupole moment element Θ_{xy} is quite large with $\Theta_{xy} = -6.2$ D \AA .

1. Introduction

The most important reactions of carbodiimides all involve nucleophilic attack across one of the imine bonds,^{1–5} and we are particularly interested in the hydrolysis and acidolysis of carbodiimides for their potential role as reactive intermediates in guanine deamination.^{6–9} Computational studies of the parent carbodiimide, $\text{HN}=\text{C}=\text{NH}$, focused on the equilibrium structure^{10,11} and dynamical aspects.^{12,13} We began ab initio studies of the hydrolysis and acidolysis of the parent carbodiimide and related heterocumulenes. We recently published results of our studies of the hydrolysis of carbodiimide^{14a,b} and carbon dioxide.^{14c–16}

In the first step of nucleophilic addition, carbodiimides and carbon dioxide form strong van der Waals complexes with nucleophiles. The bonding in these complexes is largely electrostatic with contributions due to H-bonding, other dipole–dipole interactions as well as dipole–quadrupole interactions.¹⁷ To better understand the electrostatic bonding in these complexes, one needs to learn about the charge distribution and the electrostatic moments of the heterocumulenes. The dipole and quadrupole moments are two pertinent properties in this context and only the dipole moment has been measured for carbodiimide to date. In this study, we present the results of a theoretical study of the quadrupole moment tensors components and of the measurable quadrupole moment tensor elements of carbodiimide. We are providing a direct comparison to carbon dioxide for which the quadrupole moment is known and well understood.^{16,18} The discussion focuses on the formulation of concepts that allow one to develop an understanding of the relation

between the electron density distribution and the quadrupole moment tensor components. The application of these concepts provides explanations of the level dependencies of the tensor components Q_{ii} which in turn allow for a clear understanding of the otherwise untactable level dependencies of the traceless quadrupole moments. The result of our analysis is a surprising conclusion about the quadrupolarities of the heterocumulenes carbon dioxide and carbodiimide.

2. Experimental Data of Carbodiimide

The structure of carbodiimide was determined recently by microwave spectroscopy;¹⁹ it is C_2 -symmetric and the r_s -structure is included in Table 1. The best available ab initio structure is that reported by Koput, Jabs, and Winnewisser.²⁰ These authors employed various levels up to the level CCSD-(T)/cc-pVQZ and obtained the best estimate for the structure by way of extrapolation to infinite basis set. King and Strope measured the IR spectrum of carbodiimide and of its deuterated isotopomer in an argon matrix at 20 K.²¹ We included their data in our table of vibrational data (Table 3 of the Supporting Information) and the assignment of these measured wavenumbers to the computed data was done as described by Daoudi, et al.²² The dipole moment of 1.90(5) Debye was determined by Birk et al. via microwave spectroscopy.²³ The quadrupolarity of carbodiimide has neither been measured nor theoretically predicted.^{12c}

3. Theoretical Methods and Computations

Quadrupole Moment Tensor Components. We chose the orientation of $\text{C}(\text{NH})_2$ as depicted in Figure 1 with the C and N atoms in the xz -plane. The C_2 -axis is aligned with the z -axis and the $\text{C}=\text{NH}$ bonds are almost collinear with the x -axis. CO_2 was aligned with the x -axis in ref. 16. The C_2 - z -axis transforms

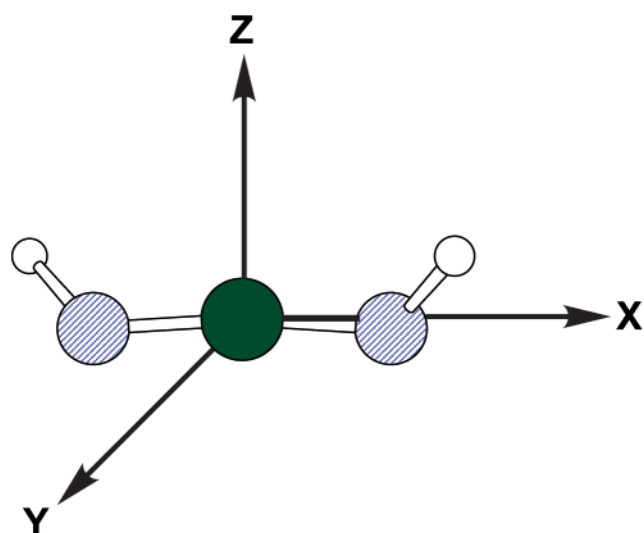
* To whom correspondence should be addressed. E-mail GlaserR@missouri.edu.

[†] Part 3 in the series "Nucleophilic Additions to Heterocumulenes." For parts 1 and 2, see refs. 14a and 16.

TABLE 1: Energies, Structure, and Atomic Charges of Carbodiimide

theoretical level	energy ^a	d(CN) ^b	d(NH) ^b	∠(NCN)	∠(HNC)	∠(HNNH)	q(C) ^c	q(N) ^c	q(H) ^c
MP2(full)-theory									
6-311G(2df,p)	-148.555602	1.223	1.012	170.70	119.05	89.58	0.624	-0.700	0.389
6-311++G(2df,p)	-148.562902	1.223	1.012	170.50	119.92	89.37	0.614	-0.703	0.396
6-311G(3df,2pd)	-148.575965	1.223	1.009	169.91	119.05	88.76	0.622	-0.699	0.388
6-311++G(3df,2pd)	-148.582292	1.224	1.009	169.99	119.73	88.89	0.611	-0.699	0.394
cc-pVTZ	-148.553063	1.223	1.007	170.26	118.97	88.75	0.593	-0.685	0.388
cc-pVTZ++	-148.563493	1.223	1.008	170.23	118.70	89.93	0.586	-0.686	0.393
QCISD(fc)-theory									
6-311G(2df,p)	-148.501429	1.223	1.013	171.65	117.04	89.93	0.658	-0.705	0.376
6-311++G(2df,p)	-148.499495	1.223	1.013	171.41	117.77	89.78	0.649	-0.707	0.383
6-311G(3df,2pd)	-148.514993	1.224	1.010	170.91	116.91	89.30	0.656	-0.703	0.375
6-311++G(3df,2pd)	-148.520355	1.224	1.010	117.06	117.46	89.39	0.647	-0.704	0.381
cc-pVTZ	-148.517260	1.225	1.010	171.37	116.64	89.50	0.627	-0.689	0.376
cc-pVTZ++	-148.521625	1.225	1.009	171.12	116.84	89.48	0.621	-0.691	0.381
exp. value¹⁹		1.22422(4)	1.00737(9)	170.630(4)	118.635(8)	88.986(5)			

^a Energies in hartrees. ^b Distances in Ångströms. ^c Charges in electrons.


Figure 1. Orientation of carbodiimide.

(x, y, z) into $(-x, -y, z)$ and integrals containing $r_i r_j$ vanish whenever the symmetry operation leads to an odd number of sign changes. For $\text{C}(\text{NH})_2$ and CO_2 , the elements Q_{xz} and Q_{yz} thus vanish. For CO_2 , the third off-diagonal element Q_{xy} also vanishes due to the C_2 y -axis, but Q_{xy} does not vanish for carbodiimide. In the chosen orientation, the diagonal element Q_{xx} characterizes the electron density distribution along the $\text{C}=\text{X}$ bonds and the diagonal elements Q_{yy} and Q_{zz} characterize the π -systems.

The unique traceless quadrupole moment Θ has the quality of a quadrupole moment tensor anisotropy. For molecules with C_2 symmetry, the traceless quadrupole moment is a tensor and there are four measurable tensor elements which can be calculated as follows

$$\Theta_{xx} = Q_{xx} - 0.5 \cdot (Q_{yy} + Q_{zz}) \quad (1)$$

$$\Theta_{yy} = Q_{yy} - 0.5 \cdot (Q_{xx} + Q_{zz}) \quad (2)$$

$$\Theta_{zz} = Q_{zz} - 0.5 \cdot (Q_{xx} + Q_{yy}) \quad (3)$$

$$\Theta_{xy} = 1.5 \cdot Q_{xy} \quad (4)$$

Carbon dioxide has just one traceless quadrupole moment Θ and it is related to the quadrupole moment tensor components by the equation $\Theta = Q_{||} - Q_{\perp} = Q_{yy} - Q_{xx}$. Molecular

quadrupole moments are on the order of 10^{-26} esu.^{17b} A list of conversion factors can be found in a recent review.²⁴ Some of the more commonly used units are related as follows: $1 \text{ esu} = 3.33564 \times 10^{-14} \text{ C m}^2$ and $1 \text{ C m}^2 = 2.99792 \times 10^{39} \text{ DÅ}$. We report quadrupole moments in units of DÅ which also are called Buckingham (B).

Theoretical Levels. We determined electron density functions $\rho(\mathbf{r})$ using restricted Hartree–Fock theory, Møller–Plesset perturbation theory, MP2(full), and quadratic configuration interaction theory, QCISD(fc).^{25,26} We previously discussed results obtained for carbon dioxide with these ab initio methods and our discussion of carbodiimide also focuses on these ab initio results. In addition, for carbodiimide we also performed density functional computations with the widely used B3LYP implementation.²⁷ The B3LYP method combines the Slater exchange functional along with corrective terms for the density gradient developed by Becke²⁸ with the correlation functional by Lee, Yang, and Parr.²⁹ The results of our DFT calculations are presented in the figures for comparison.

Several basis sets were employed and they include the 6-31G* and 6-31G** basis sets³⁰ and the 6-311G** and 6-311++G** basis sets.^{31,32} The step from double- ζ to triple- ζ valence description provides a major improvement. Further improvement is achieved by additional flexibility in the number and the type of the polarization functions and we have considered four options;³³ 6-311G(2d,p), 6-311G(2df,p), 6-311G(3d,2pd), and 6-311G(3df,2pd). Finally, all of these basis sets are augmented with diffuse functions. The valence double- ζ basis set D95V(d,p)³⁴ and some of Dunning’s correlation-consistent basis sets cc-pVnZ³⁵ also were employed. The cc-pVTZ basis set is comparable to the 6-311G(2df,p) basis set in terms of basis functions but features many more primitives. These basis sets also were used with augmentation by diffuse functions (with the exponents employed in the Pople basis sets). This procedure differs from the usual diffuse function augmentation of the cc-pVnZ basis sets which adds one diffuse function of each type (including d- and f-functions).

All structures were optimized with each method and each basis set.³⁶ Total energies, optimized structures and atomic charges determined at selected levels are given in Table 1. The natural population analysis (NPA)³⁷ was employed to determine atomic charges. The respective dipole moments, quadrupole moment tensor components and traceless quadrupole moment tensor elements Θ_{xx} , Θ_{yy} , Θ_{zz} , and Θ_{xy} are given in Table 2.

TABLE 2: Dipole Moment,^a Quadrupole Moment Tensor Components, and Measurable Quadrupole Moments of Carbodiimide^b

theoretical level	$\mu(z)$	Q_{xx}	Q_{yy}	Q_{zz}	Q_{xy}	Θ_{xx}	Θ_{yy}	Θ_{zz}	Θ_{xy}
MP2(full)-theory									
6-311G(2df,p)	2.047	-15.922	-16.735	-17.348	-4.146	1.120	-0.101	-1.019	-6.219
6-311++G(2df,p)	2.088	-16.344	-17.243	-17.882	-4.376	1.219	-0.130	-1.089	-6.564
6-311G(3df,2pd)	1.916	-15.780	-16.862	-17.462	-3.999	1.382	-0.241	-1.141	-5.998
6-311++G(3df,2pd)	1.979	-16.313	-17.292	-17.903	-4.186	1.285	-0.184	-1.100	-6.279
cc-pVTZ	2.023	-16.105	-16.912	-17.502	-4.088	1.103	-0.109	-0.994	-6.133
cc-pVTZ++	2.013	-16.293	-17.027	-17.632	-4.134	1.036	-0.064	-0.972	-6.201
QCISD(fc)-theory									
6-311G(2df,p)	2.087	-16.627	-16.636	-17.205	-4.114	0.293	0.280	-0.573	-6.172
6-311++G(2df,p)	2.127	-16.994	-17.072	-17.671	-4.329	0.378	0.261	-0.638	-6.494
6-311G(3df,2pd)	1.968	-16.467	-16.740	-17.306	-3.989	0.556	0.146	-0.702	-5.983
6-311++G(3df,2pd)	2.029	-16.965	-17.114	-17.684	-4.159	0.434	0.210	-0.644	-6.239
cc-pVTZ	2.066	-16.837	-16.779	-17.340	-4.081	0.222	0.310	-0.532	-6.121
cc-pVTZ++	2.054	-16.881	-16.891	-17.469	-4.121	0.299	0.285	-0.584	-6.182
exp. values ²³	1.90(5)								

^a Dipole moments in D. ^b Quadrupole moments in DÅ.

Complete versions of Tables 1 and 2 and a table with the vibrational data are provided as Supporting Information.

In the figures, we ordered the data as much as possible with increasing basis set quality from left to right. Double- ζ basis sets are located on the left and triple- ζ basis sets are on the right. The diffuse-function augmented basis set always follows immediately to the right of the same basis set without that augmentation. Within the two main blocks, the basis sets are ordered in a way that reflects more flexibility in the basis functions (e.g., V95D vs 6-31G*) or more primitives (e.g., cc-pVDZ vs 6-31G* or V95D), or more sets of polarization functions, and more types of polarization functions.

Convergence versus Direct Comparison to Experiment. Only the structure, the dipole moment and some of the vibrational frequencies of carbodiimide were measured (vide supra). In such a situation, one can proceed in several ways to ensure theoretical results of high accuracy. The purely theoretical approach would entail the gradual improvement in the theoretical level until all properties have converged. This approach is rigorous but it is only practical for very small molecules. The more practical approach relies on the establishment of the accuracy of a theoretical level and this approach requires experimental data. We are using a combination of these approaches. The experimental data available for the isoelectronic CO₂ are employed to establish the accuracies of a variety of hierachically ordered theoretical levels and the assumption is made that the same accuracies can be claimed in calculations of C(NH)₂.

Our study of CO₂¹⁶ showed that MP2 and QCISD calculations in conjunction with triple- ζ basis sets reproduce the experimental CO bond length to within 0.01 Å. The original measurement of the quadrupole moment of CO₂ gave $\Theta = -14.34 \pm 0.7 \times 10^{-40}$ C m² ($-4.3 \pm 0.2 \cdot 10^{-26}$ esu)³⁸ and subsequent refinement gave $\Theta = -14.27 \pm 0.61 \times 10^{-40}$ C m² (4.278 DÅ).³⁹ We showed that the correlated levels with triple- ζ basis sets were able to reproduce this value.¹⁶

In this paper, we will show that the quadrupole moment tensor components of carbodiimide and carbon dioxide have almost the same theoretical level and basis set dependencies. Any method that successfully reproduces the known quadrupole moment of CO₂, can be expected to yield reliable results for C(NH)₂ as well. The figures display the data for C(NH)₂ and they may be compared to the respective figures of ref. 16 for CO₂.

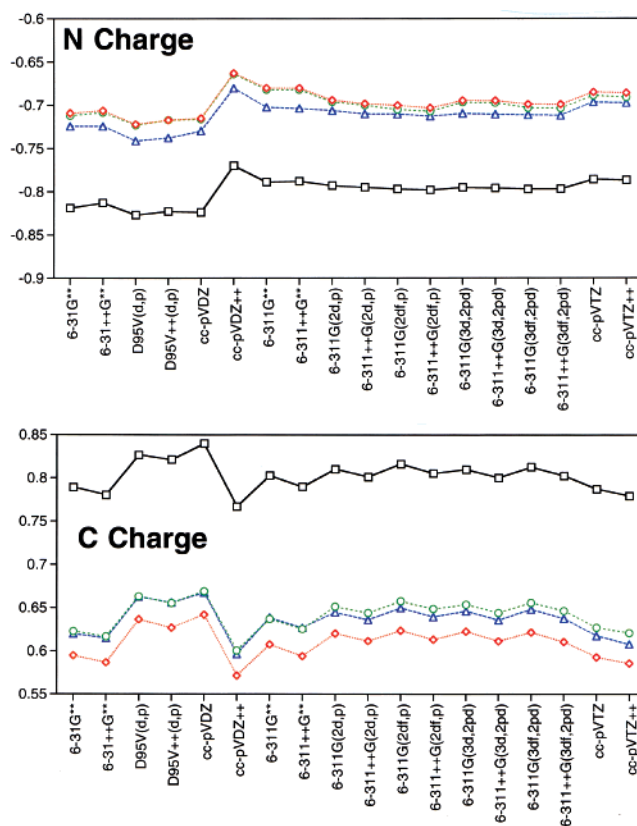


Figure 2. Theoretical level and basis set dependencies of the N (top) and C (bottom) charges in carbodiimide. (□ = RHF, ◇ = MP2, ○ = QCISD, Δ = B3LYP).

4. Results and Discussion

4.1. Computed Structures and Atomic Charges. The theoretical level dependency of the CN bond length in carbodiimide, like the CO bond length in CO₂, is correlated with the atomic charges. RHF underestimates the CN bond length by -0.010 to -0.021 Å, whereas MP2 and QCISD structures agree almost perfectly with experiment (Table 1). The RHF charges for carbodiimide range from $+0.77$ to $+0.84$ for C and from -0.77 to -0.83 for N (Figure 2). At the correlated levels the electron density is more delocalized resulting in a less positive C atom (from $+0.59$ to $+0.66$) and a less negative N atom (-0.66 and -0.72). The RHF method gives highly

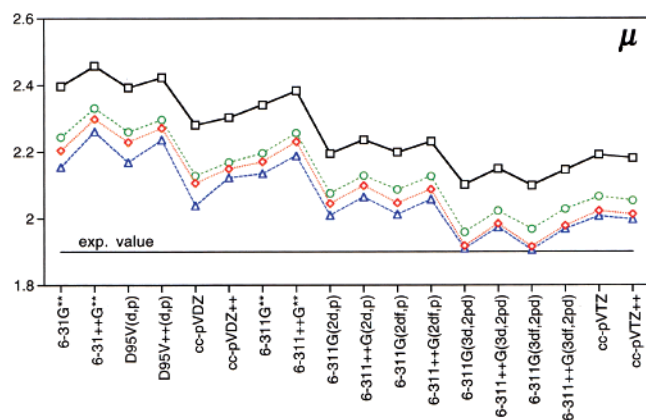


Figure 3. Theoretical level and basis set dependencies of the dipole moment of carbodiimide in Debye. (\square = RHF, \diamond = MP2, \circ = QCISD, Δ = B3LYP).

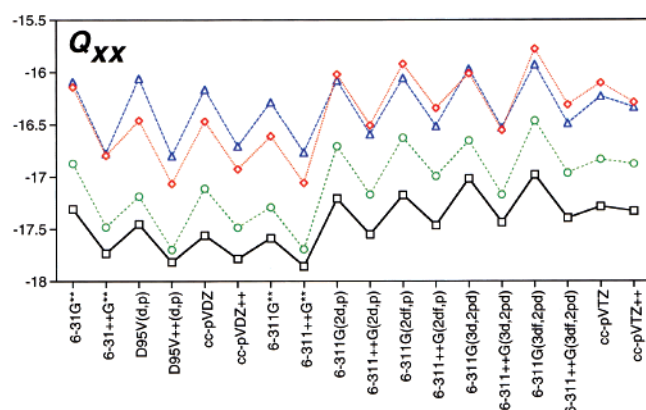


Figure 4. Theoretical level and basis set dependencies of the Q_{xx} tensor component of carbodiimide in Debye Ångströms. (\square = RHF, \diamond = MP2, \circ = QCISD, Δ = B3LYP).

charged atoms and leads to overestimation of the electrostatic attraction between C and N. Electron correlation via the MP2 or QCISD methods corrects the problem. Basis set effects on the CN bond length are much less pronounced than the theoretical model dependency. For the correlated methods, the experimental structure is essentially obtained through the use of triple- ζ basis sets with the inclusion of diffuse functions.

4.2. Dipole Moment. The dipole moment shows significant theoretical level and basis set dependencies and the computed value is higher than the experimental value of 1.90(5) D at all levels (Figure 3). The best values were obtained with the correlated methods in concert with triple- ζ basis sets with polarization and diffuse functions. The use of a third d-function in the correlation treatment yields a calculated dipole moment within experimental error. The dipole moment of carbodiimide is largely due to the NH bonds. The dipole moment of "linear" carbodiimide ($\angle(\text{NCN}) = 180^\circ$, no contribution from CN bonds) is 2.044 D at RHF/4-31G, whereas the optimized C_2 structure has a dipole moment of 2.165 D at the same level.^{12a}

The atomic charge on N is directly correlated to the dipole moment of carbodiimide (Figure 2). RHF overestimates the dipole moment by 0.28 to 0.54 D. The MP2 and QCISD methods allow for charge relaxation at N (Figure 2), and the calculated μ values are less exaggerated.

4.3. Quadrupolarity. The quadrupole moment tensor components are given in Table 2 and trends are revealed by graphical analysis (Q_{xx} in Figure 4, Q_{yy} and Q_{zz} in Figure 5). All tensor components of carbodiimide are negative and indicate that, on r^2 -weighted average, the negative charge distribution is farther

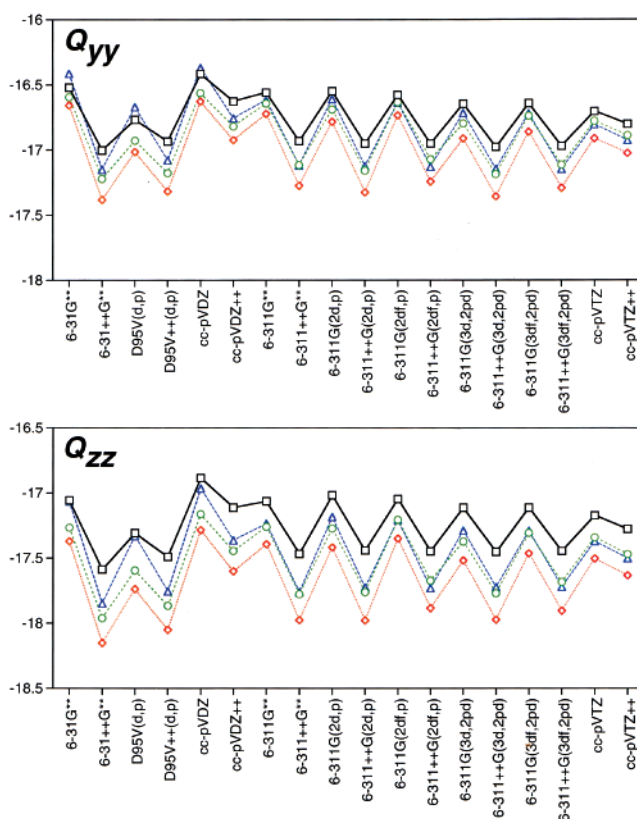


Figure 5. Theoretical level and basis set dependencies of the Q_{yy} (top) and Q_{zz} (bottom) tensor components of carbodiimide in Debye Ångströms. (\square = RHF, \diamond = MP2, \circ = QCISD, Δ = B3LYP).

removed from the molecular center of the nuclear charges. Hence, in all three independent directions carbodiimide is characterized by the quadrupolarity $\{- + -\}$.

Rationalization of Diagonal Elements Q_{yy} and Q_{zz} . Carbodiimide is a cumulene with a near-cylindrical π -cloud along the N-C-N skeleton. To understand the $\{- + -\}$ quadrupolarity of the Q_{yy} and Q_{zz} tensor components it is useful to consider just the $\text{N}=\text{C}=\text{N}$ fragment. The MO representation of each π -system of $\text{C}(\text{NH})_2$ is as depicted schematically in part (a) of Figure 6. The electron density of the $\text{N}=\text{C}=\text{N}$ fragment is very much like that of carbon dioxide, that is, it is highly cylindrical and the representation shown in part (b) of Figure 6 is quite appropriate. Approaching $\text{C}(\text{NH})_2$ along the y - or z -axes involves passing through the negative region of the π -cloud, then the positive area of the nuclei, and then the second negative region of the π -cloud. The $\{- + -\}$ quadrupolarity of Q_{yy} and Q_{zz} is intuitively easy to grasp and a negative value has to result since the nuclei do not contribute to Q_{yy} and very little to Q_{zz} . For carbon dioxide, the nuclei contribute neither to Q_{yy} nor to Q_{zz} . It is important to realize that Q_{yy} and Q_{zz} are not only a function of the π -MOs but also contain contributions from the σ -MOs (neglected in Figure 6).

Rationalization of Diagonal Element Q_{xx} . We rationalize the negative value of the Q_{xx} tensor component of $\text{C}(\text{NH})_2$ as in the case of CO_2 .¹⁶ The explanation, however, requires a deeper insight because intuition might lead one to expect $\{+ - +\}$ quadrupolarity for Q_{xx} due to the positively charged peripheral H atoms. The Q_{xx} value of the $\text{N}=\text{C}=\text{N}$ fragment would indicate a $\{- + -\}$ quadrupolarity as for $\text{O}=\text{C}=\text{O}$. Consider the electron density distributions associated with two degenerate sp_x hybrid orbitals centered at a distance x_0 from the center of nuclear charge. The positions $x_0 + \Delta x_0$ and $x_0 - \Delta x_0$ are equidistant from the position x_0 . The volume elements

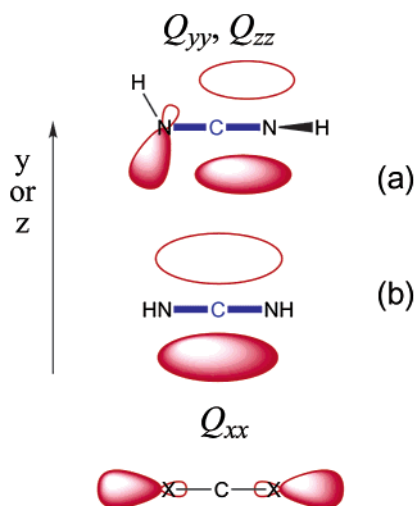


Figure 6. Rationalization of the quadrupole moment tensor components.

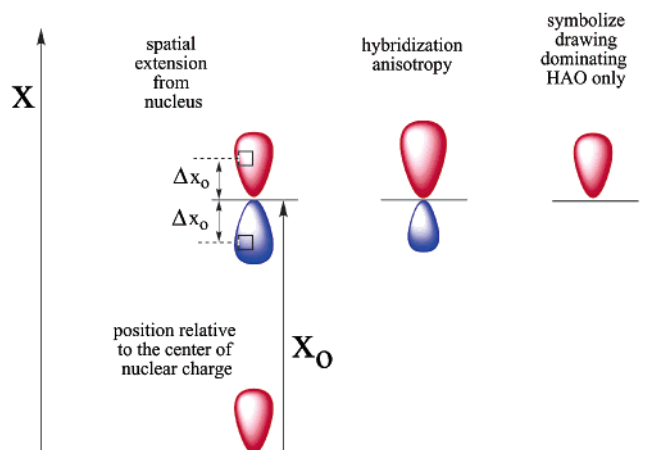


Figure 7. Effects of position, spatial extension and hybridization anisotropy of atomic orbitals on the diagonal element Q_{xx} .

at positions $x_0 - \Delta x_0$ and $x_0 + \Delta x_0$ contribute $-|\rho(r)| \cdot (x_0 - \Delta x_0)^2$ and $-|\rho(r)| \cdot (x_0 + \Delta x_0)^2$, respectively, and their combined contribution to Q_{xx} is $-|\rho(r)| \cdot (2x_0^2 + 2\Delta x_0^2)$. An atom-centered electron density component that is symmetrical with regard to that atom contributes to Q_{xx} (Figure 7) and the contribution increases (i) with the distance of the atom from the center of the nuclear charge and (ii) with the spatial extension of the orbital (influences Δx_0 range).

At the next level of sophistication one might consider differences in the shapes of the approximate sp hybrid orbitals. One of the hybrid orbitals might be more spatially extended and this *hybridization anisotropy* is illustrated to the right in Figure 7. Note that the electron density around the N atom will contribute a negative amount to Q_{xx} even if the electron density around that atom is not polarized in the x -direction. In reality, the electron density at the N atoms does show a polarization in the x -direction to place more electron density behind the N atom and this hybridization anisotropy *increases* Q_{xx} . The N-sp-type hybrid orbital of the N lone pair in $C(NH)_2$ is spatially more extended than the respective N-sp-type hybrid orbital of the $C=N$ bond because the electrons involved in CN bonding are more contracted due to the higher attraction term in the one-electron core Hamiltonian of the CN bonding MO. Extended basis sets are required to adequately describe this N atom anisotropy because the greater spatial extension of the density

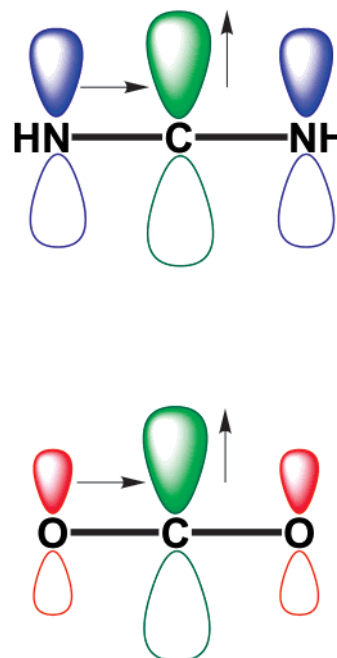


Figure 8. Schematic illustration of the increased spatial extension of electron density in the proximity of carbon.

in the N lone pair region requires the use of greater contribution of the outer C p-basis function(s). The C atom's contribution to Q_{xx} is *negative* as well. The C nucleus does not contribute at all and the electron density associated with the sp_x orbitals gives rise to a negative contribution to Q_{xx} (even though the C-atom is *positively* charged). The Q_{xx} value of $C(NH)_2$ would be dominated by the contributions due to the N atoms, because $\langle x_0 \rangle$ is large for the N atoms, whereas $\langle x_0 \rangle = 0$ for the C atom. The quadrupolarity Q_{xx} of the $N=C=N$ fragment of carbodiimide can therefore be understood as the result of three effects: (i) atom positioning x_0 , (ii) hybrid orbital spatial extension Δx , and (iii) hybridization anisotropy.

The addition of a proton to each end of the $N=C=N$ dianion results in a Q_{xx} value that is more positive than Q_{xx} for just the $N=C=N$ dianion. But how much more positive? The Q_{xx} value of CO_2 is between -19 and -20 DÅ and we can use this value as an approximation for Q_{xx} of the $N=C=N$ fragment of $C(NH)_2$. The H atoms in $C(NH)_2$ are only 1.9 Å away from the center of charge and this is not nearly far enough to overcome the already large $\{- + -\}$ quadrupolarity. The Q_{xx} value of $C(NH)_2$ is -16 to -18 DÅ (Figure 4) and only about 3 DÅ less negative than the corresponding value for CO_2 .¹⁶

Theoretical Model Dependency of Diagonal Elements Q_{ii} . The theoretical model dependency of Q_{xx} is pronounced, up to 1.5 DÅ (Figure 4), and correlation always results in a less negative Q_{xx} value. We can explain this result with the atomic charges and the set of guidelines developed in Figure 7. Correlation decreases the negative charge on the N atoms and the negative contribution to Q_{xx} due to atom positioning (x_0) is markedly decreased. The decrease of electron density at N further diminishes the negative contribution to Q_{xx} from hybrid orbital spatial extension (Δx_0) and hybridization anisotropy.

The calculated Q_{yy} and Q_{zz} values are -16.5 to -17.5 and -17 to -18 DÅ, respectively (Figure 5). The effects of electron correlation are much less pronounced than in the case of Q_{xx} ; Q_{yy} and Q_{zz} are only slightly more negative at the RHF level. The effects of correlation on Q_{yy} and Q_{zz} can be explained by the atomic charges and the ideas illustrated by Figure 8. Electron density becomes more spatially extended as it is transferred from

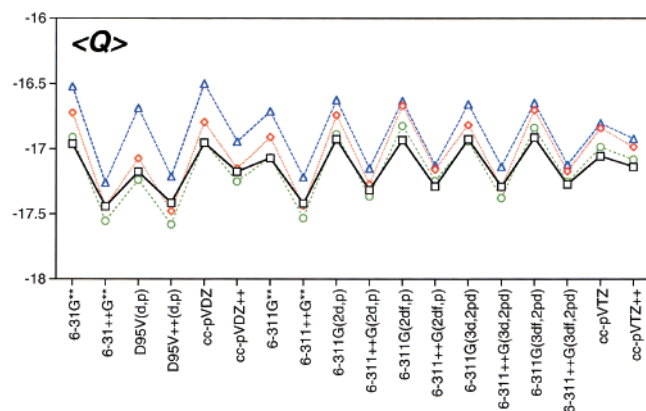


Figure 9. Theoretical level and basis set dependencies of the average of the diagonal elements $\langle Q_{ii} \rangle$ of carbodiimide in Debye Ångströms. (\square = RHF, \diamond = MP2, \circ = QCISD, Δ = B3LYP).

N to C and Q_{yy} and Q_{zz} become more negative. The electron density at N is less contracted than at O and the arrows in Figure 8 are meant to indicate this electron density shift. Figure 8 also illustrates why the Q_{yy} and Q_{zz} values of carbodiimide are 2–3 DÅ more negative than for carbon dioxide.¹⁶

The Q_{xx} , Q_{yy} , and Q_{zz} values of carbodiimide (Figures 4 and 5) have very similar theoretical level and basis set dependencies as CO_2 .¹⁶ This gives us confidence that our best theoretical levels will give highly accurate values for $\text{C}(\text{NH})_2$ because we have demonstrated that these same levels reproduce the experimental quadrupole moment of CO_2 . Figure 4 also supports our explanation of the negative Q_{xx} value of $\text{C}(\text{NH})_2$ via the $\text{N}=\text{C}=\text{N}$ fragment. Figure 5 shows that the Q_{yy} and Q_{zz} values of $\text{C}(\text{NH})_2$ are almost the same and this finding suggests that the π -electron density is nearly cylindrical as in the case of CO_2 . Figures 4 and 5 show in a compelling fashion that the Q_{xx} , Q_{yy} , and Q_{zz} values all decrease by about 0.5 DÅ with the addition of diffuse functions at most theoretical levels and with most basis sets.

Off-Diagonal Element. Q_{xy} is smaller than the diagonal elements by a factor of 4 and it ranges from -4.0 to -4.8 DÅ. There is a small theoretical level dependency for Q_{xy} and a more significant basis set dependency with respect to the inclusion of diffuse functions (vide supra). The Θ_{xy} element of the measurable quadrupole moment is a scalar multiple of Q_{xy} (equation 4).

Average of the Diagonal Elements $\langle Q_{ii} \rangle$. The $\langle Q_{ii} \rangle$ value ranges from -16.5 to -17.5 DÅ, it is about 1 DÅ more negative than for CO_2 ¹⁶ and Figure 9 shows hardly any theoretical level dependency. This theoretical level “independence” is due to the cancellation of two systematic errors: At RHF the Q_{xx} values always are too negative while the Q_{yy} and Q_{zz} values always are not negative enough.

Measurable Quadrupole Moments. The four quadrupole moment tensor elements of carbodiimide are given in Table 2 and the theoretical level dependencies are illustrated in Figure 10. Our study of CO_2 ¹⁶ revealed that QCISD in conjunction with polarized triple- ζ basis sets reproduces the experimental value. The Θ_{xx} value of $\text{C}(\text{NH})_2$ ranges from -1 to 1.5 DÅ with the most accurate QCISD values hovering around 0 – 0.5 DÅ. The Θ_{yy} value is between 0 and 0.8 DÅ with the best QCISD data around 0.5 DÅ and the Θ_{zz} values span from 0 to -1 DÅ with the most reliable QCISD numbers around -0.5 DÅ. The RHF data give the most negative Θ_{xx} values and the most positive Θ_{yy} and Θ_{zz} values. This is a direct result of the underestimation of the Q_{xx} tensor component (vide supra). The

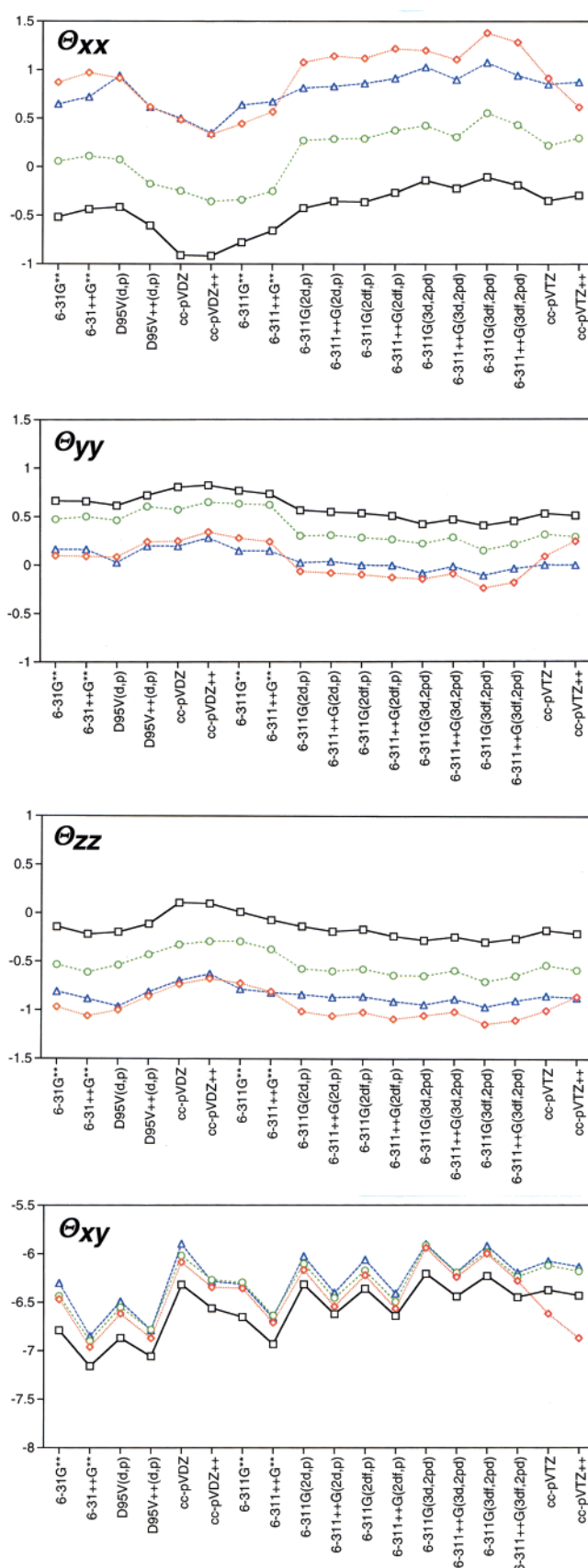


Figure 10. Theoretical level and basis set dependencies of the measurable quadrupole moment tensor elements Θ_{xx} (top), Θ_{yy} (middle-top), Θ_{zz} (middle-bottom), and Θ_{xy} (bottom) of carbodiimide in Debye Ångströms. (\square = RHF, \diamond = MP2, \circ = QCISD, Δ = B3LYP).

theoretical level dependency is much greater for Q_{xx} than for Q_{yy} and Q_{zz} . Thus, from eqs 1–3 the theoretical level depend-

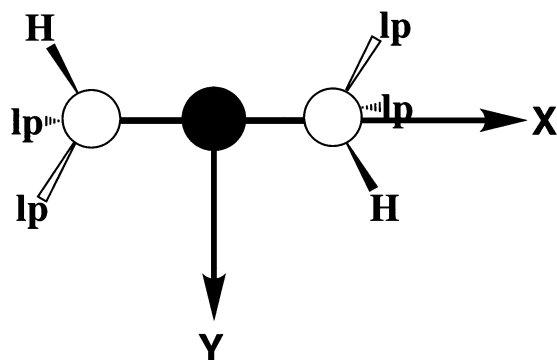


Figure 11. Schematic illustration to aid the discussion of the electron density anisotropy of the N atom.

encies of Θ_{xx} , Θ_{yy} , and Θ_{zz} become obvious. The small magnitudes of the Θ_{xx} , Θ_{yy} , and Θ_{zz} quadrupole moments should make them desirable targets for experimentalists because calculations cannot predict with complete certainty whether these values will be negative or positive.

The only nonzero off-diagonal tensor element is Θ_{xy} , and its value is between -6 and -7.3 DÅ. There is a very small theoretical level dependency with the RHF values being marginally more negative than the correlated values.

Θ_{xy} has to do with the anisotropy around the N atoms caused by the H atoms. To illustrate this point qualitatively, one might consider the idealized case shown in Figure 11. The structure in Figure 11 is “ C_{3v} symmetric” and perfectly staggered. The structure can be seen as an idealized presentation of the resonance form of carbodiimide with polar C(+)-N(-) bonds. It becomes obvious that the lone pairs in the xz -plane do not contribute to Θ_{xy} . Next, one needs to realize that the electron densities associated with the N-H bonds and the other lone pair contribute to Θ_{xy} with opposite sign. So, the fact that $|\Theta_{xy}| \neq 0$ means that the electron densities of the N-H bond and the lone pair are different and the fact that $\Theta_{xy} < 0$ means that the spatial orbital extension of the lone pair is larger.

5. Conclusions

Our previous results for carbon dioxide suggested and the results presented here for carbodiimide corroborate that the MP2 methods in conjunction with well-polarized triple- ζ basis sets provides a cost-effective and accurate method for the estimation of correlation effects on quadrupole moments. The B3LYP data for carbodiimide show that this density functional method performs as well or better than MP2 and this insight allows for further cost-savings in the computations of accurate quadrupole moments.

The quadrupolarities of carbodiimide and carbon dioxide are very different. The quadrupolarity of CO_2 is defined as $\Theta = Q_{xx} - 0.5 \cdot (Q_{yy} + Q_{zz}) = Q_{||} - Q_{\perp}$ and both the experimental and the best theoretical values are -4.3 DÅ. The definition of Θ for CO_2 is equivalent to the definition of Θ_{xx} for $\text{C}(\text{NH})_2$. Coupling this with the fact that $\text{C}(\text{NH})_2$ and CO_2 are isoelectronic, one might expect high Θ_{ii} quadrupolarities for carbodiimide. However, this is *not* the case. The Q_{xx} value for CO_2 is about -19 DÅ and Q_{xx} for $\text{C}(\text{NH})_2$ is about -17 DÅ and this difference causes Θ_{xx} to be 2 DÅ less negative for $\text{C}(\text{NH})_2$ compared to CO_2 . The Q_{\perp} value of CO_2 is -14.25 DÅ and the average of the Q_{yy} and Q_{zz} values of $\text{C}(\text{NH})_2$ is -17 DÅ. This difference causes Θ_{xx} to be another 2.75 DÅ less negative for $\text{C}(\text{NH})_2$ compared to CO_2 . Overall, the O/NH-replacement results in a reduction of $\Theta_{xx}(\text{CO}_2) = -4.3$ DÅ by approximately 4.75 DÅ to near zero for $\Theta_{xx}(\text{C}(\text{NH})_2)$. The same logic applied

to eqs 2 and 3 explains why Θ_{yy} and Θ_{zz} also are near zero. Only the off-diagonal quadrupole moment element Θ_{xy} is quite large. Thus, our study of $\text{C}(\text{NH})_2$ predicts Θ_{xy} to be the only quadrupole moment tensor element with a significant magnitude and our best estimate of its value is $\Theta_{xy} = -6.2$ DÅ.

The dipole and the quadrupole moments of carbodiimide are related to the N-H bond polarity. This is in stark contrast to CO_2 where the quadrupolarity is due to the C-O bond polarity. This difference should affect aggregation geometries, approach paths and the structures of precoordination complexes in nucleophilic additions. The high magnitude of Θ_{xy} in conjunction with the presence of a dipole moment should render all of these aggregates more bound than in the respective case of carbon dioxide.

We have formulated concepts to develop an understanding of the relation between the electron density distribution and the quadrupole moment tensor components. Most chemists understand MO theory but many have little or no conceptual knowledge of quadrupoles. To make the connection between properties of molecular orbitals and quadrupole moments builds conceptual understanding.

Acknowledgment. This research was supported by grants from the MU Research Council and the National Institutes of Health (NIGMS GM61027). M.L. is the recipient of a Natural Sciences and Engineering Research Council of Canada scholarship, type B.

Supporting Information Available: Complete Tables 1 and 2, and a Table 3 with vibrational data of carbodiimide. This material is available free of charge at <http://pubs.acs.org>.

References and Notes

- (1) Khorana, H. G. *Chem. Rev.* **1953**, *53*, 145.
- (2) Kurzer, F.; Douraghi-Zadeh, K. *Chem. Rev.* **1967**, *67*, 107.
- (3) Williams, A.; Ibrahim, I. T. *Chem. Rev.* **1981**, *81*, 589.
- (4) (a) Schimzu, T.; Seki, N.; Taka, H.; Kamigata, N. *J. Org. Chem.* **1996**, *61*, 6013. (b) Schuster, E.; Hesse, C.; Schumann, D. *Synlett* **1991**, *12*, 916. (c) Olah, G. A.; Wu, A.; Farooq, O. *Synthesis* **1989**, *7*, 568.
- (5) (a) Slebiada, M. *Tetrahedron* **1995**, *51*, 7829. (b) Ibrahim, I. T.; Williams, A. *J. Chem. Soc., Perkin Trans. 2* **1982**, 1459.
- (6) (a) Caulfield, J. L.; Wishnok, J. S.; Tannenbaum, S. R. *J. Biol. Chem.* **1998**, *273*, 12689. (b) Burrows, C. J.; Muller, J. G. *Chem. Rev.* **1998**, *98*, 1109.
- (7) (a) Glaser, R.; Son, M.-S. *J. Am. Chem. Soc.* **1996**, *118*, 10 942. (b) Glaser, R.; Rayat, S.; Lewis, M.; Son, M.-S.; Meyer, S. *J. Am. Chem. Soc.* **1999**, *121*, 6108. (c) Glaser, R.; Lewis, M. *Org. Lett.* **1999**, *1*, 273.
- (8) (a) Suzuki, T.; Yamaoka, R.; Nishi, M.; Ide, H.; Makino, K. *J. Am. Chem. Soc.* **1996**, *118*, 2515. (b) Suzuki, T.; Kanaori, K.; Tajima, K.; Makino, K. *Nucleic Acids Symp. Ser.* **1997**, *37*, 313. (c) Suzuki, T.; Yamada, M.; Kanaori, K.; Tajima, K.; Makino, K. *Nucleic Acids Symp. Ser.* **1998**, *39*, 177.
- (9) Lucas, L. T.; Gatehouse, D.; Shuker, D. E. G. *J. Biol. Chem.* **1999**, *274*, 18 319.
- (10) Nguyen, M. T.; Riggs, N. V.; Radom, L.; Winnemisser, M.; Winnemisser, B. P.; Birk, M. *Chem. Phys.* **1988**, *122*, 305.
- (11) Bertran, J.; Oliva, A.; Jose, J.; Duran, M.; Molina, P.; Alajarin, M.; Leonardo, C. L.; Elguero, J. *J. Chem. Soc., Perkin Trans. 2* **1992**, 299.
- (12) (a) Nguyen, M. T.; Ha, T.-K. *J. Chem. Soc., Perkin Trans. 2* **1983**, 1297. (b) Lehn, J. M.; Munsch, B. *Theor. Chim. Acta* **1968**, *12*, 91. (c) The study in ref. a reports the quadrupole moment tensor components for carbodiimide at the RHF/4-31G level. These numbers are obviously in error because the Q_{zz} value given is positive. In the present study, all 42 levels of theory give a highly negative Q_{zz} value of approximately -17 to -18 DÅ.
- (13) Pracna, P.; Winnemisser, M.; Winnemisser, B. P. *J. Mol. Spectrosc.* **1993**, *162*, 127.
- (14) (a) Lewis, M.; Glaser, R. *J. Am. Chem. Soc.* **1998**, *120*, 8541. (b) Lewis, M.; Glaser, R. *Chem. Eur. J.* **2002**, *8*, 1934. (c) Lewis, M.; Glaser, R., submitted.
- (15) (a) Leorting, T.; Tautermann, C.; Kroemer, R. T.; Kohl, I.; Hallbrucker, A.; Mayer, E.; Liedl, K. R. *Angew. Chem., Int. Ed.* **2000**, *39*,

892. (b) Hage, W.; Liedl, K. R.; Hallbrucker, A.; Mayer, E. *Science* **1998**, 279, 1332. (c) Liedl, K. R.; Sekusak, S.; Mayer, E. *J. Am. Chem. Soc.* **1997**, 119, 3782.
- (16) Glaser, R.; Wu, Z.; Lewis, M. *J. Mol. Struct.* **2000**, 556, 131.
- (17) (a) Buckingham, A. D. *Quarterly Rev. (London)* **1959**, 8, 183. (b) Molecular quadrupole moments are on the order of 10 magnitudes larger than nuclear quadrupole moments (ref 17a). Specifically, the nuclear quadrupole moment of ^{14}N atom is $3.22 \times 10^{-49} \text{ Cm}^2$ (area $2.01 \times 10^{-30} \text{ m}^2$ and elementary charge $1.602 \times 10^{-19} \text{ C}$) or $9.65 \times 10^{-10} \text{ D}\text{\AA}$; see Mills, I.; Cvitas, T.; Homann, K.; Kalley, N.; Kuchitsu, K. *Quantities, Units and Symbols in Physical Chemistry*, 2nd ed.; International Union of Pure and Applied Chemistry, Physical Chemistry Division and Blackwell Science: Cambridge, Mass., 1993.
- (18) For related studies of the quadrupolarity of conjugated systems, see also: (a) Glaser, R.; Lewis, M.; Wu, Z. *J. Mol. Model.* **2000**, 6, 86. (b) Glaser, R.; Chen, G. S. *Chem. Mater.* **1997**, 9, 28.
- (19) Jabs, W.; Winnewisser, M.; Belov, S. P.; Lewen, F.; Maiwald, F.; Winnewisser, G. *Mol. Phys.* **1999**, 97, 213.
- (20) Koput, J.; Jabs, W.; Winnewisser, M. *Chem. Phys. Lett.* **1998**, 295, 462.
- (21) King, S. T.; Strope, J. H. *J. Chem. Phys.* **1971**, 54, 1289.
- (22) Daoudi, A.; Pouchan, C.; Sauvatre, H. *J. Mol. Struct.* **1982**, 89, 103.
- (23) Birk, M.; Winnewisser, M.; Cohen, E. A. *J. Mol. Spectrosc.* **1989**, 136, 402.
- (24) Spackman, M. A. *Chem. Rev.* **1992**, 92, 1769.
- (25) (a) Szabo, A.; Ostlund, N. S. *Modern Quantum Chemistry: Introduction to Advanced Electronic Structure Theory*, MacMillan Publishing Co., Inc.: New York, New York, 1982. (b) Hehre, W. L.; Schleyer, R. D.; Radom, L. P. v. R.; Pople, J. A. *Ab Initio Molecular Orbital Theory*; John Wiley & Sons: New York, New York, 1986.
- (26) (a) Head-Gordon, M.; Pople, J. A.; Raghavachari, K. *J. Chem. Phys.* **1987**, 87, 5968. (b) Hampel, C.; Peterson, K. A.; Werner, H.-J. *Chem. Phys. Lett.* **1992**, 120, 1.
- (27) Koch, W.; Holthausen, M. C. *A Chemist's Guide to Density Functional Theory*, 2nd ed.; Wiley-VCH: New York, New York, **2001**.
- (28) Becke, A. D. *Phys. Rev. A* **1988**, 38, 3098.
- (29) Lee, C.; Yang, W.; Parr, R. G. *Phys. Rev. B* **1988**, 37, 785.
- (30) 6-31G* and 6-31G**: (a) Hehre, W. J.; Ditchfield, R.; Pople, J. A. *J. Chem. Phys.* **1972**, 56, 2257. (b) Frisch, M. M.; Pietro, W. J.; Hehre, W. J.; Binkley, J. S.; Gordon, M. S.; DeFrees, D. J.; Pople, J. A. *J. Chem. Phys.* **1982**, 77, 3654. (c) Hariharan, P. C.; Pople, J. A. *Theor. Chimica Acta* **1973**, 28, 213.
- (31) 6-311G**: (a) Krishnan, R.; Binkley, J. S.; Seeger, R.; Pople, J. A. *J. Chem. Phys.* **1980**, 72, 650. (b) McLean, A. D.; Chandler, G. S. *J. Chem. Phys.* **1980**, 72, 5639.
- (32) Diffuse functions: Clark, T.; Chandrasekhar, J.; Schleyer, P. v. R. *J. Comput. Chem.* **1983**, 4, 294.
- (33) Multiple polarization functions: Frisch, M. J.; Pople, J. A.; Binkley, J. S. *J. Chem. Phys.* **1984**, 80, 3265.
- (34) D95V basis set: Dunning, T. H.; Hay, P. J. in *Modern Theoretical Chemistry*, Schaefer, H. F. III, Ed., Vol. 3, p 1. Plenum Press: New York, 1976.
- (35) cc-pVnZ basis sets: Wilson, A.; Mourik, T.; Dunning, T. H. *J. Mol. Struct. (THEOCHEM)* **1997**, 388, 339, and references therein.
- (36) Frisch, M. J.; Trucks, G. W.; Schlegel, H. B.; Gill, P. M. W.; Johnson, B. G.; Robb, M. A.; Cheeseman, J. R.; Keith, T.; Petersson, G. A.; Montgomery, J. A.; Raghavachari, K.; Al-Laham, M. A.; Zakrzewski, V. G.; Ortiz, J. V.; Foresman, J. B.; Cioslowski, J.; Stefanov, B. B.; Nanayakkara, A.; Challacombe, M.; Peng, C. Y.; Ayala, P. Y.; Chen, W.; Wong, M. W.; Andres, J. L.; Replogle, E. S.; Gomperts, R.; Martin, R. L.; Fox, D. J.; Binkley, J. S.; Defrees, D. J.; Baker, J.; Stewart, J. P.; Head-Gordon, M.; Gonzalez, C.; Pople, J. A. *Gaussian 94*, Revision C.3; Gaussian Inc.: Pittsburgh, PA, 1995.
- (37) (a) Glendening, E. D.; Reed, A. E.; Carpenter, J. E.; Weinhold, F. *NBO Version 3.1*. (b) Glendening, E. D.; Weinhold, F. *J. Comput. Chem.* **1998**, 19, 628, and references therein.
- (38) Buckingham, A. D.; Disch, R. L.; Dunmur, D. A. *J. Am. Chem. Soc.* **1968**, 90, 3104.
- (39) Graham, C.; Imrie, D. A.; Raab, R. E. *Mol. Phys.* **1998**, 1, 49.